In Vivo Evaluation of The Novel Nanocomposite Porous 3D Scaffold in a Rabbit Model

**Saffanah Khuder Mahmood[1,2], Intan Shameha Binti Abdul Razak[1],
Sahar Mohammed Ibrahim[4], Loqman Mohamed Yusof[5], Adamu Abdul Abubakar[6],
Zaid Khudhur Mahmood[7] and Zuki Abu Bakar Zakaria[1,3*]**

[1]Department of Veterinary Preclinical Sciences, Faculty of Veterinary Medicine, Universiti Putra Malaysia (UPM), 43400, Serdang, Selangor Darul Ehsan, Malaysia; saffanh.jeber@gmail.com, intanshameha@upm.edu.my
[2]Department of Veterinary Anatomy, Faculty of Veterinary Medicine, University of Mosul, Mosul, Iraq;
[3]Laboratory of Molecular Biomedicine, Institute of Biosciences, Universiti Putra Malaysia (UPM), 43400, Serdang, Selangor Darul Ehsan, Malaysia; zuki@upm.edu.my
[4]Department of Surgery and Theriogenology, College of Veterinary Medicine, University of Musol, Musol, Iraq; sahar2011973@yahoo.com
[5]Department of Companion Animal Medicine and Surgery, Faculty of Veterinary Medicine, Universiti Putra Malaysia (UPM), 43400, Serdang, Selangor Darul Ehsan, Malaysia; loqman@upm.edu.my
[6]Department of Veterinary Surgery and Radiology, Usmanu Danfodiyo University, Sokoto, Nigeria; babaji32002@gmail.com
[7]Department of Veterinary Clinical Studies, Faculty of Veterinary Medicine, Universiti Putra Malaysia (UPM), 43400, Serdang, Selangor Darul Ehsan, Malaysia; zaid.jeber@gmail.com

Abstract

Objectives: To evaluate, *In Vivo*, the developed porous nanocomposite scaffold from cockle shell nanopowder for segmental bone defect (SBD) repair. **Methods/Statistical Analysis:** Complete critical bone defect (2cm) made on the shaft of radial bone of adult male New Zealand White rabbit. Then implanted with scaffold and assessed for 8 weeks by means of radiography, grossly and biochemistry. The rabbits were divided into 4 groups: Group A (control), Group B (implanted by scaffold 5211), Group C (implanted by 5211GTA+Alginate) and Group D (implanted by 5211PLA). **Findings:** Radiographic examination showed new trabecular bone formation that signifies the bone healing/regeneration. This occurred in the defects edge as well as in the middle within one month which involved osteogenesis that moved within the central region and margins of the scaffold implant. This was attained with negligible tissue responses to a foreign body which was seen through biochemistry analyses (ALP and Ca+2). Grossly, after 8 weeks post-implantation the quantity of mature bone increased forming whole bone. The new bone tissue that was produced was successively matured within time as anticipated with increased mature cortical bone development and regeneration. **Application/Improvements:** This work signifies key development in the healing of artificial bone grafts and suggests that the biomaterial of the grafted scaffold possess significant potential when regeneration of bone is necessary.

Keywords: *In Vivo*, Nanocomposite, Porous, Rabbit, Scaffold

1. Introduction

Repair is the standard mammalian response to significant organ injury. It is typically characterized by closure of the wound through contraction and scar formation. Generally this means that the organ in question loses most or all of its functionality. Regeneration on the other hand is characterized by restoration of the normal structure and

---

function of the organ[1]. Usual bone comprises of inorganic and organic portions being in uninterrupted exchange to each other for formation of bone and resorbing, i.e. the procedure of remodeling. The remarkable ability of bone tissues in repairing itself often fails in situations when a fracture is found to be either too complicated or a defect too large to be bridged that often results in a non-union healing[2]. Severe fractures (critical bone defects) leading to non-union of wounded bone and resection of bone linked with removal of tumor does not healed through natural healing response of the body, it thus need medical involvement. The critical bone defects can be covered by soft tissues but reconstruction of the bone itself may be difficult. The damage or malfunction of organs and tissues as a result of injury or trauma or aging is a major cause of concern in the care of human health[3].

Investigational work on a critical-size bone part restoration using polymer compounds in weight-bearing settings is restricted. Critical-size bone deformity models in weight-bearing settings are tough in constructing, because the size of the deformity needs differs from species to species, which makes the investigation habitually lacking in excellence[4]. Transplantation is the most widely used treatment to overcome the deficiencies associated with tissue repair. Autografting is transplantation using healthy tissue harvested from the patient, whereas allograftingutilizes tissue taken from a separate donor. Despite the widespread use of transplantation, there are several shortcomings of this treatment[5].

Tissue engineering provides an alternative to transplantation and prosthesis, with the potential to overcome the limitations of these treatments[6]. Tissue engineering is defined as the scientific principles application in the production of living tissues through the use of bioreactors, cells, scaffolds, growth factors, or a combination[7]. The scaffold can be implanted single-handedly to prompt host cell colonization to the wounded position and tissue restoration, or it can be seeded with cells and/or growth factors and serve to control the release and targeting of these treatments. Bone tissue engineering shows promise as an alternative to repair critical bone defects. Accordingly, bone tissue engineering was developed in both scope and significance in biomedical engineering. It signifies the linkage of fast growths in cellular and molecular biology in the way and materials, chemical and mechanical engineering in another way[8].

Bone tissue engineered constructs ought to eventually possess two major purposes when implanted *in vivo*: 1) Give structural support to neo tissue and 2) Promote osteo induction, which means simplistically, promoting movement of Mesenchymal stem cells, differentiation and osteo genesis which leading to formation of new bone[9]. Biomaterials can offer a solution to these difficulties. Different inorganic biomaterials, for example tricalcium phosphate (TCP), natural coral (NC) and hydroxyapatite (HA) have been broadly utilized as BMPs carriers. Bioglasses and metals are encompassed in the group of inorganic carrier materials. These biomaterials share the characteristic of being immunologically inactive, osteoconductive, partly or wholly biodegradable and robust mechanically[10]. Nanoparticles (NPs) are particles that have at least one dimension between 1 and 100 nm in size[11]. The size gives them unique properties which inversely proportional to their surface/volume ratio chemical reactivity[12].

This study used a composite scaffold that is fabricated from the cockle shell-derived $CaCO_3$ aragonite nanoparticles, gelatin, dextran and dextrin as a basis for tissue engineering. Gelatin has gotten a reasonable consideration over the past few years due to its outstanding biocompatibility, degradation into physiological end-products and appropriate interaction with macromolecules and cells[13,14]. Practically, the cockle shell permeable forms are used as bone scaffolds to ascertain an upgraded bone ingrowth and osseointegration. To be used efficiently in weight bearing parts, the mechanical properties of the cockle shell-derived $CaCO_3$ aragonite porous scaffold body have to be enhanced[15,16]. In the setting of bone tissue engineering it is also significant to note that there are different literature view on the association between Glutaraldehyde (GTA) crosslinking and mineralization. In some studies GTA crosslinking revealed to induce calcification in some *in vivo* research. Nevertheless it has been revealed that GTA can also compromise mineralization in collagen and a glycosaminoglycan (GAG) scaffolds[17]. Furthermore, the pore arrangement of the scaffold requires to be controlled in terms of penetrability and size of pore. As a result of optimizing the desire requirements, coating design of the porous scaffold was suggested. By coating with plastic polymer layer, the fragility of the porous scaffold is likely to be overcome[18].

Saffanah Khuder Mahmood, Intan Shameha Binti Abdul Razak, Sahar Mohammed Ibrahim, Loqman Mohamed Yusof, Adamu
Abdul Abubakar, Zaid Khudhur Mahmood and Zuki Abu Bakar Zakaria

Numerous polymers such as poly (Llactic) acid (PLLA), poly (caprolactone) (PCL), alginate, gelatin and poly-b-hydroxybutyrate have been investigated as potential coating system for bioceramic scaffolds[19]. Normal polymers can offer inherent patterns for cell adhesion, growth and stimulate an immune reaction as a result of their biocompatibility. Similarly, the microstructures of the normal polymers are very organized and contain extracellular substance which performance as provisional extracellular matrix (ECM) for effective bone regeneration. Therefore, natural polymer coating over the ceramic scaffold is a healthier method for making mechanically sound scaffold for orthopedic applications[20]. The choice of an appropriate animal model is an important factor taken into consideration. An animal having larger structure ought to be selected for this experiment for example rabbit because the size-to-weight proportion, the axial loading design of the limbs look like those of human being, a high bone turnover rate as well as for displaying similarities in bone density and fracture toughness comparative to the human bones[21]. The aim of this study is to evaluate the actual tissue biocompatibility of the smart scaffolds fabricated (unpublished data) with and without coated framework as bone substitute as well as its potentials in producing an appropriate response in regards to promoting new bone tissue formations within the time frame of study.

2. Materials and Methods

2.1 Experimental Animals, Anesthesia and Postoperative Follow-up

A total of 16 adult male New Zealand White rabbits, age 8-11 months, and weighing 2-4 Kg were used in this research. They were separated into 4 groups of 4 animals each according to the keeping duration of 8 weeks and labeled as group A, B, C and group D. Group A rabbits were had a part of their radial bone (2 cm) (mid shaft) removed by a bone cutter and the critical size defect left empty without implantation as a control. Group B rabbits were implanted with non-coated scaffolds (scaffold 5211). Group C rabbits were implanted with scaffold 5211 with cross linking and coated with alginate ($5211_{GTA+Alginate}$). Group D rabbits were implanted with scaffold 5211 coated with PLA (5211_{PLA}). All the scaffolds were prepared by the freeze drying method.

The study protocol was approved by the Institute of animal care and use committee (IACUC), Faculty of Veterinary Medicine, Universiti Putra Malaysia (UPM) (UPM/IACUC/AUP-R015/2015). They were housed and maintained at constant temperature and provided with commercial feed rabbit chow ad libitum and water. An overnight (12 hours) food and water deprivation period preceded the surgery. The animals were anesthetized using the ketamine hydrochloride 35mg/kg B.W I/M and xylazine hydrochloride 3-5mg/kg B.W I/M and anaesthetic maintenance carried out using Halothane and O_2.

2.2 The Scaffolds

The scaffolds prepared as described in (unpublished data) by freeze drying method and coated framework were used in this experiment. For the *in vivo* post-implantation evaluation, scaffolds 5211, $5211_{GTA+Alginate}$ and 5211_{PLA} were used. The criteria for selecting particular scaffold were based on experimental observation of porosity, mechanical strength, and Young's modulus and degradation manner. The novel cockle shell-derived $CaCO_3$ aragonite nanocomposite scaffolds were cut into cylindrical shape corresponding to the size of radial bone defect with 4 mm diameter and 20 mm length (Figure 1). For group B: the rabbits were implanted by scaffold 5211. Similarly for group C: the rabbits were implanted by scaffold $5211_{GTA+Alginate}$ and group D: the rabbits were implanted by scaffold 5211_{PLA}.

2.3 Surgical Procedure

The surgeries were all performed under aseptic conditions in the small animal surgery room located within the facilities of the Veterinary Teaching Hospital, UVH, and UPM. Prior to surgery, the animals were weighed and checked for general health conditions. Initial sedations and inductions were performed with Isoflurane via gas mask at a flow rate of 5% at 0.5 lit/min of oxygen flow rate. The sedation was maintained with Isoflurane at a flow rate of 1-1.5% in 0.5 lit/min of oxygen flow rate throughout the entire surgical procedure. Following onset of sedation, skin was done by shaving the lower limbs of the animals prior to washing with alcohol and prepped with providone-iodine solution before being covered under surgical drapes prior to placing the animals on a towel to maintain appropriate temperature. The vital signs of the animals were also monitored throughout
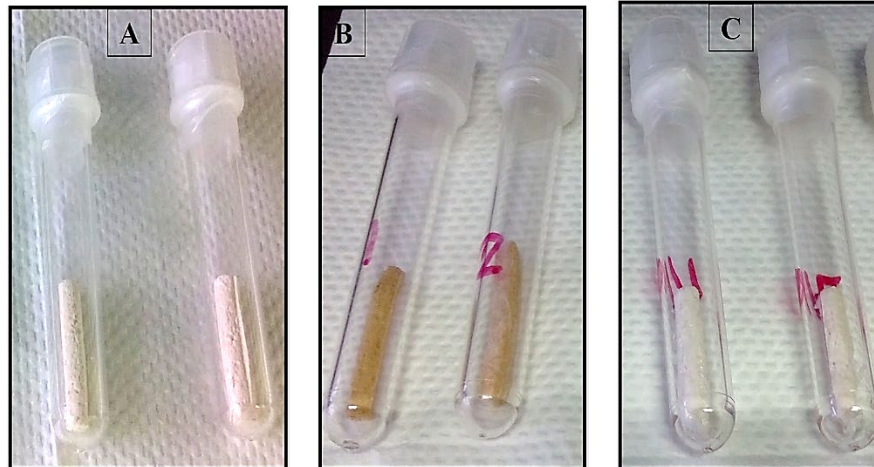
Figure 1 (A-C).   Photographs show scaffolds 5211 (A), $5211_{GTA+Alginate}$ (B) and 5211_{PLA} (C) after drying in the freeze dryer machine, which ready to be used for implantation.

the surgery. Following skin preparation, an approximately 3 cm incision was made in the skin at craniomedial surface over the radial bone on the proximal third of the left forelimb through the skin and fascia to expose the shift of the radial bone. A twenty mm critical size defect (CSD) was manually created on the radial bone using bone cutter. The defect was examined immediately after removal of the bone chip, while the right limb was left to serve as a negative control without defect for comparative pur-

poses. The scaffolds were inserted into the defect area in a gentle press fit manner till it was completely fixed into the defect without the help of bone plate (Figure 2). The wound incision was then carefully sutured back with 3-0 (Antibacterial with Irgacare MP**) (Polyglactin 910) absorbable surgical sutures (Undyed Braided) (Coated VICRYL*Plus-ETHICON*) using simple continuous suturing method. Surgical bandages were then draped around the limb in order to maintain the hygiene of the
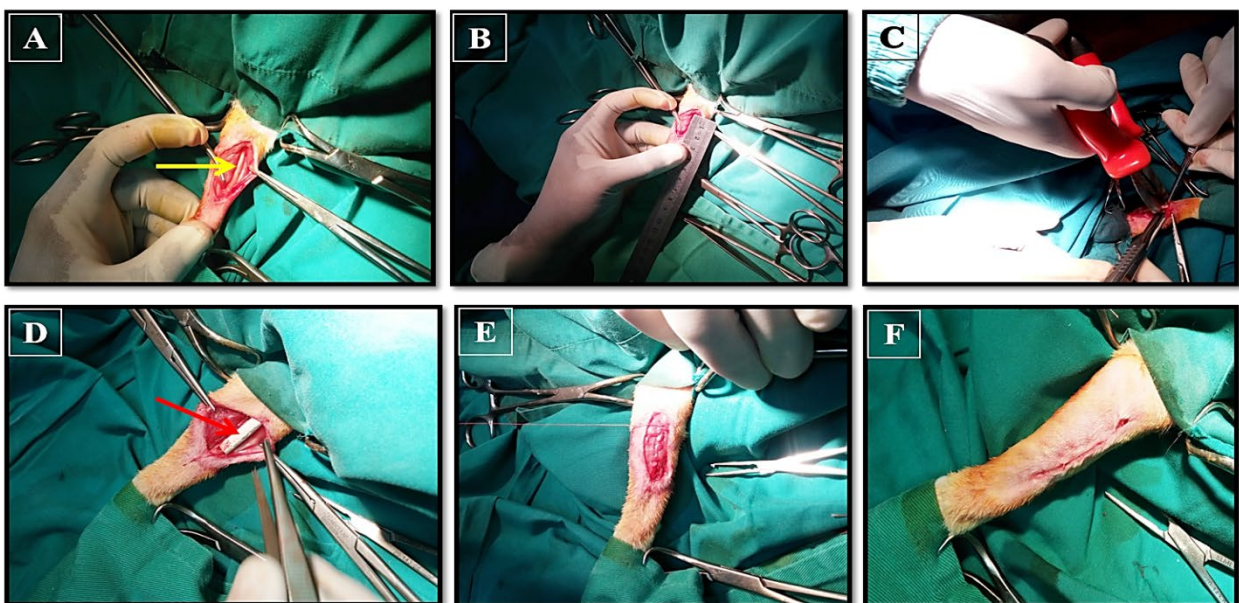

Figure 2 (A-F).   Photographs show the surgical procedure of creating a defect in radial bone (yellow arrow) and scaffold implantation into the defect area in a rabbit model. Note that the defect is well fixed with the sterilized 3D scaffolds (red arrow).

surgical site post-surgery. The animals were then sent for radiographic imaging prior to recovery. Radiographs were taken at day 1, week's 4 and 8 post-implantation to examine the formation of new bone tissue. The rabbits were euthanized on week8 post-implantation by giving an overdose of the sodium pentobarbital (Dolethal1mg/kg intravenously I/V; 1ml=182mg pentobarbital). The bone samples were then collected for gross examination.

2.4 Post-Operative Care

Post-operative care involved close monitoring of the animals for any signs of possible complications such as surgical wound infections or tears. The animals were given subcutaneous injections of postoperative prophylactic antibiotics Baytril (5% w/v 1 ml/10 kg B.W) and postoperative analgesic Tramadol hydrochloride (5mg/kg B.W) for 3 consecutive days. The animals were also allowed full weight bearing activity as well as access to water and rabbit chow ad libitum. At day 3, the surgical bandage was removed and the surgical wounds were periodically checked for healing and signs of inflammation.

2.5 Post-Implantation Evaluation

2.5.1 Radiographic Examination

Post-operative radiographs were taken during the anesthesia in antero-posterior and lateral views of the radial bone immediately after the surgery, 4 and 8weeks post-implantation using a Shimadzu mobile X-ray machine and Carastream Direct View Vita CR for image processing. Radiological incorporation, possible resorption of host bone and growth of new bone were assessed round the implant and at the bone-implant intersections. The evaluation of the union margin between the new bone tissue formation and the host tissue by radiographic examination was distinguishable, the bridging callus and state of scaffold well-being were examined and recorded.

2.5.2 Serum Biochemistry

Blood serum were collected from the ear vein into plain vacutainer tubes for serum biochemical assays. Alkaline phosphatase (ALP) and calcium (Ca^{+2}) levels were measured in the serum pre-implantation, at week 1, 2, 3, 4 and 8 post-implantation for non-implantation rabbits (control) and implantation rabbits (treated groups) as osteoblastic expression of the cells and markers further explain the capability of the synthetic bone in achieving regeneration of bone *in vivo*. The activities of alkaline phosphatase and Ca^{+2} were assessed using a 902 Hitachi automated clinical chemistry analyzer.

2.5.3 Clinical Observations and Gross Examination

The rabbits used were able to tolerate the surgical processes very well, no single animal was lost at the surgical process. The animals were euthanized in accordance to the research protocol and the guidelines provided by the central animal laboratory. All animals recuperated and their limbs function normally and the animals were moving normally in few days after the surgery. The animal remain in a good condition during the study (no infections, good appetite, active, etc.), as they were examined every day. Mortality was not recorded throughout the experiment. Following euthanasia at week 8 post-implantation, the radial bones of both limbs of the animals were harvested. The bones were cleaned by removing the surrounding soft tissues and the scaffold implanted sites were grossly examined prior to be viewed. The bones were then viewed under Nikon SMZ 1500/Japan stereomicroscope to illustrate any changes in bone formation in different stages during this short period of bone being, and through the complete healing when compared with normal radial bone.

2.6 Statistical Analysis

First of all, the quantifiable outcomes were evaluated using Explore for normality of data then one-way analysis of variance (ANOVA) and Kruskal-wallis test. The results were shown as mean ± standard error (SE). Post hoc test were calculated for significant values (p<0.05) using Tukey's multiple comparison test. All descriptive and inferential statistical analyses was conducted using Excel version 2013, SPSS version 21.0, 22.0 and 23.0.

3. Results

3.1 Radiographic Examination

Bone absorbs the X-Ray beam according to the amount of calcium available in that particular bone. Accordingly, there was a range of greyscale in the X-Ray image. This range of greyscale was used to specify the status of the bone. The radiographic images of the defects taken after surgery for all the groups revealed that images obtained

immediately post-surgery showed a clear radiolucent defect with low radiodensity at the defect sites on all groups on the left limbs of the animals. The implanted scaffolds were also visible within the defined edges of the defect site at close examination. Radiological images demonstrate very well the bone developing phenomena around the implant, a robust new bone callus shielded the implant's sides as was established by histological study (accepted data for publication).

Group B: The defect was clearly seen with well-defined edges and the implant material was also clearly seen in the early postoperative phase (day 1 post-implantation) (Figure 3A). At 4 weeks post-implantation, radiographic examination revealed new bone formation at proximal and distal part of the defect site as indicated by the radio opaque implant scaffold. However, the entire implant became radio opaque at 4 but at 8 weeks post-implantation, new bone was not wholly constructed as indicated by the radiolucent area within the defect, left the radial bone nonunion (Figure 3B).

Group C: The similar result was found in the early postoperative phase (day 1 post-implantation). The defect was clearly seen with well-defined edges and the implant material was also clearly seen at 2 weeks post-implantation (Figure 4A). Four weeks after implantation,

the broad formation of bone was seen over the defect implanted with scaffold $5211_{GTA+Alginate}$ which occupied the deform space (Figure 4B). Postoperatively, all animals move freely and were weights bearing on the operated limb. The radiographic examination showed that significant new bone has form at 8 weeks post-implantation and the implanted scaffolds boundaries was smooth and the scaffold borders were indistinct. The callus formation was seen during this period over the both proximal, middle and distal radial-scaffold junction. The implant scaffold became more radio opaque indicating the new bone formation was progressing (Figure 4C). The implant borders were well defined indicating the remodeling process was in progress, although the complete formation of new bone was seen at each ends of the defect at 8 weeks, the radio density of the implanted scaffolds has further increased. The critical defect area was almost completely repaired during this time.

Group D: The implanted scaffolds were clearly seen in plain radiograph of rabbit's radial bone in the early postoperative phase (day 1 post-implantation) (Figure 5A). The defect was clearly seen with well-defined edges and the implant material was also clearly seen at 2 weeks post-implantation (Figure 5B). At 4 weeks post-implantation, radiographic investigation showed formation of new bone at proximal part of the defect site and directed to
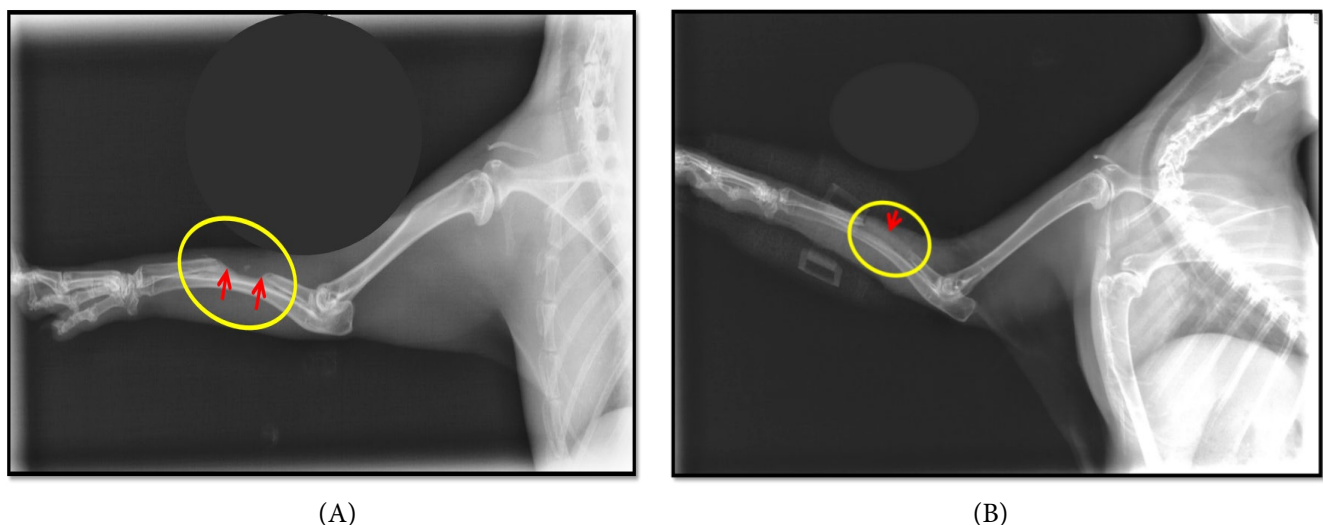

(A)   (B)

Figure 3 (A&B). Radiographs of the radial bone defect post-implantation for group B at day 1 post-implantation (A) reveals the well-defined edges and the implant material is clearly seen (yellow circle and red arrow) and after 8 weeks post-implantation (B) show the small radio opaque area at the implant site and indistinct border of the radial bone due to new bone formation. Note that the new bone was not completely constructed as indicated by the radiolucent within the defect (yellow circle and red arrows).
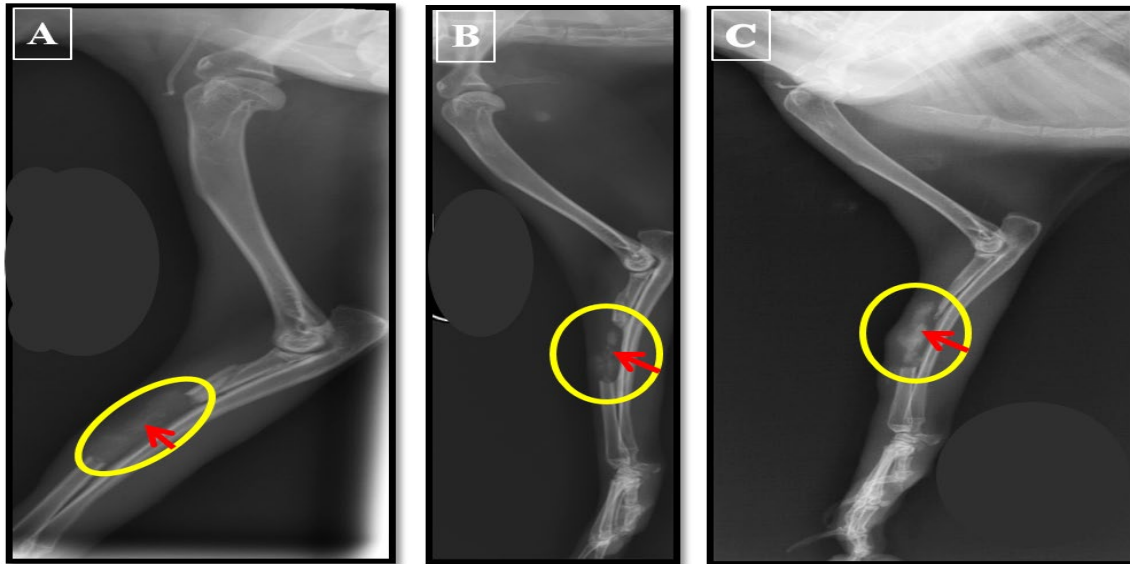
Figure 4 (A-C). Radiographs of the radial bone defect post-implantation of group C, (A) after 2 weeks, the implant material was clearly seen, (B) after 4 weeks, the very small radio opaque area was seen over the defect implanted, (C) after 8 weeks post-implantation shows the very extensive bone formation radio opaque area at the implant site and indistinct border of the radial bone due to new bone formation.
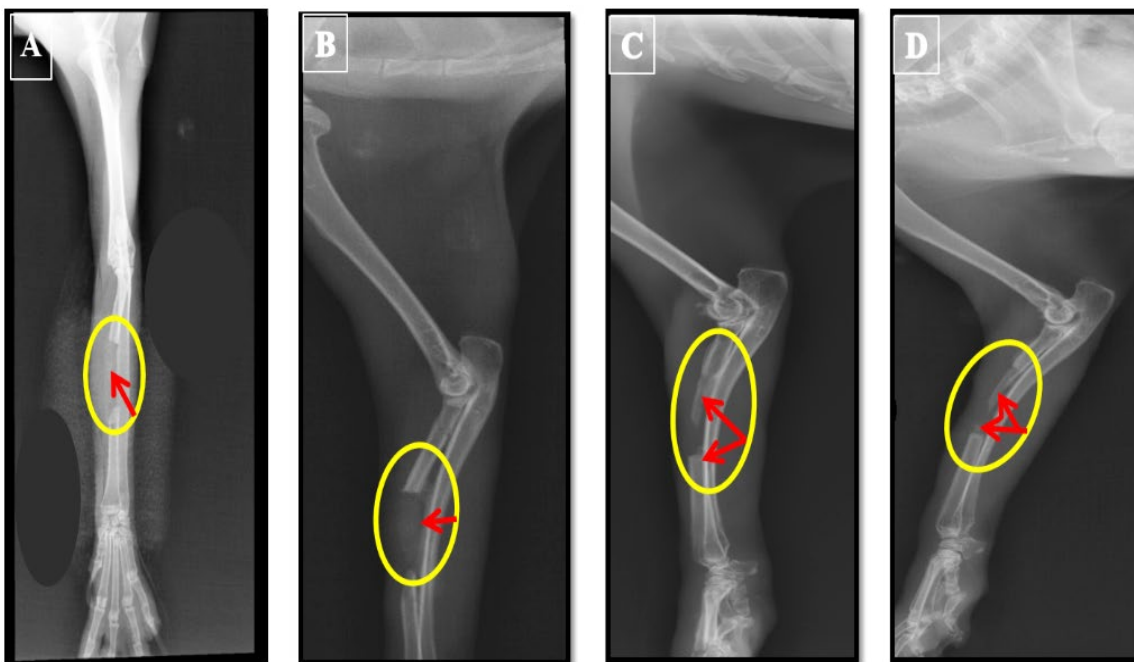

Figure 5 (A-D). Radiographs of the radial bone defect post-implantation of group D, (A) after 1st day post-implantation, (B) after 2nd week the implant material was clearly seen, (C) after 4th week and (D) after 8th week post-implantation show the very extensive bone formation radio opaque area at the implant site and indistinct border of the radial bone due to new bone formation.

distal part as indicated by the radio opaque implant scaffold (Figure 5C). However, the entire implant became radio opaque at 4 weeks but at 8 weeks post-implantation, the new bone was not entirely constructed as indicated by the radiolucent area within the defect, left the radial bone nonunion (Figure 5D).
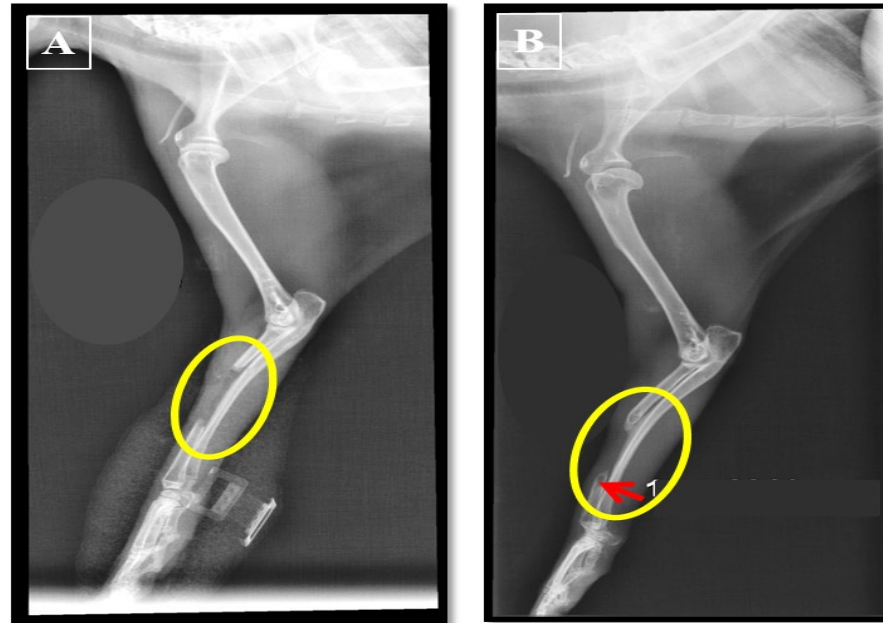
Figure 6 (A & B).   Radiographs of the radial bone defect of group A (Control group) (A) after 1st day post-surgery (yellow circle), (B) after 8th week show the very small radio opaque area at the defect site (yellow circle and red arrow). Note that the new bone was not completely constructed as indicated by the radiolucent within the defect.

In the defects for **Group A** (control group) (Figure 6A), a very small area at the defect site was seen radio opaque at 8 weeks post-implantation, and the two end of the radial bone were distinct clearly (Figure 6B). However, the new bone was not completely constructed as indicated by the radiolucent area within the defect, left the radial bone nonunion.

3.2 Serum Biochemistry

3.2.1 Alkaline Phosphatase Activity (ALP) Analysis

ALP activity was measured as an indicator of osteoblastic activity. Variations in the entire ALP level according to the bone repair procedure were alike to normal bone fractures healing. In normal conditions of the bone repair, total ALP concentration rise to the peak level at 3 weeks post-surgery and then progressively declined[22]. The results in this study revealed that the total ALP changes have almost the similar pattern as compared to normal fracture healing; however the extent of alteration was considerably different between group A, B, C and D. In general, group A revealed a significant rise in the total ALP value as compared to the group B, C and D from 1 to 8 weeks post-implantation (Figure 7). Nevertheless,

the range of changes was significantly higher ($P<0.05$) for group A (control) as compared to other groups within pre-implantation (zero day) and post-implantation. For treated groups, the total ALP was decreased after 3 weeks but maintained lower than the group a (control group) until the week 8 post-implantation. In both groups B and D, the total ALP concentration increased 1st week post-implantation to reaching a peak at 3rd weeks post-implantation and then progressively declined, and the amount of change in the ALP concentration was clearer in group A. The concentration of ALP in both groups has not reverted to the early level at 8 weeks post-implantation, even though the value has decreased from the highest level. The increase in the ALP concentration as equated to the preoperative values were noted from 1 to 8 weeks post-implantation; after the maximum (at week 3 post-implantation), the value declined. The fluctuating pattern of ALP in group B, C and D are almost similar. In control animals, the ALP activity remained high.

However a gradual increase in ALP levels were observed in the nanocomposite scaffold implanted groups from 45 IU/L prior to surgery to a maximum value of 55 IU/L at week 3 before gradually decreasing. The ALP levels of the control scaffold group however showed a slight increase in ALP levels at week 1 followed by a slight
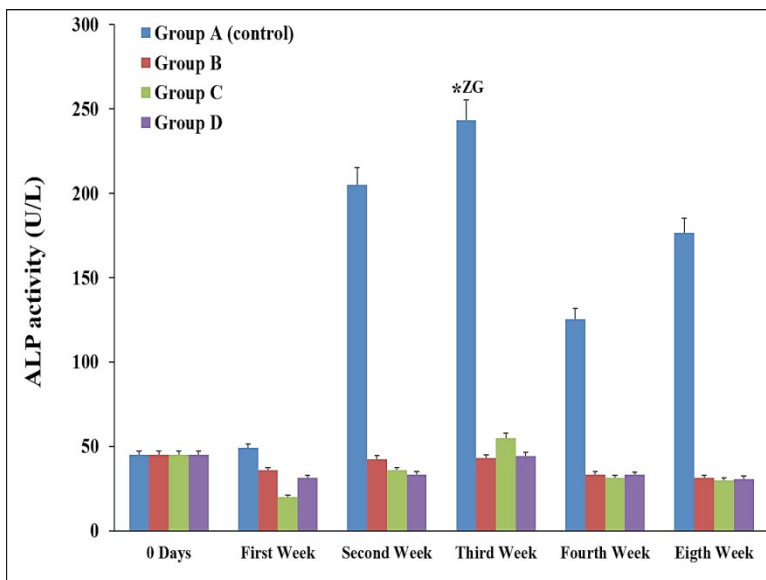
Figure 7. The graph shows the value of total alkaline phosphatase (ALP) in fourth groups at different time intervals post-implantation. *ZG Significant difference was observed between groups and as compared to zero day at $p<0.05$.

decrease in the values by week 4 which was then followed by a gradual increase in the values by week 8 (Figure 7).

3.2.2 Calcium Analysis

The calcium (Ca^{+2}) was measured as a sign to the mineralization of bone tissue formation. The value of the serum calcium declined considerably and lingered low for a two weeks in both groups B, C and D, and then improved to usual level or over at the end of the post-implantation period (Figure 8). However, the range of calcium value change was significantly difference at ($P<0.05$) between groups. The changes of the calcium value in implanted groups indicating the progression of bone formation. The increases in calcium concentration equated to the preop-
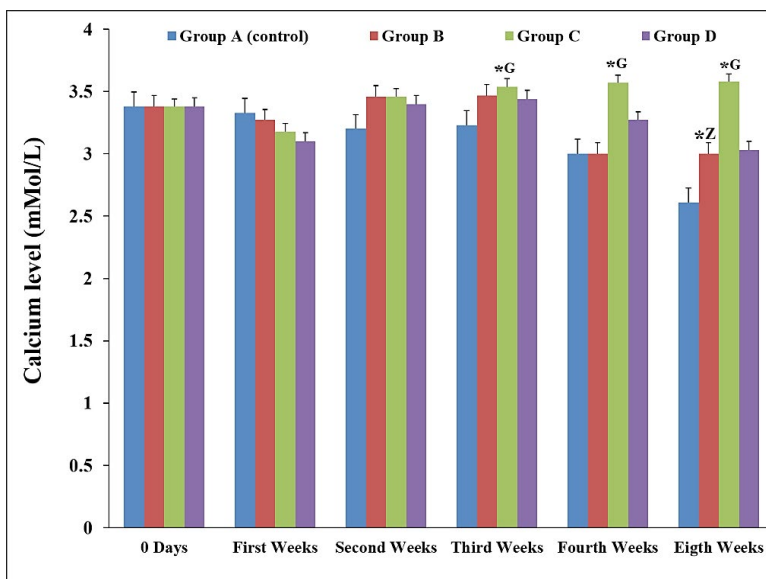

Figure 8. The graph shows the value of calcium (Ca^{+2}) in fourth groups at time intervals post-implantation. *ZG Significant difference was observed between groups and as compared to zero day at $p<0.05$.

erative values were taken into consideration from 1 to 8 weeks after implantation with the high peak was at 8 week post-implantation.

Obvious changes in calcium levels were observed in the nanocomposite scaffold and the control groups. The range of calcium levels in the nanocomposite scaffold implanted groups 3-3.58 IU/L, while the control group 2.61-3.33 IU/L during experimental period (8 weeks).

3.3 Gross Examination

The results revealed that all the rabbits survived from surgery intervention, and sign of inflammation was not seen or adverse tissue response was detected around the implants. Grossly it was revealed that the radial bone defects in all groups implanted with scaffolds were healed with different levels. Gross examination of group B rabbits (implanted with scaffold 5211), the clinical union was observed that the rabbits exhibit painless mobility over the proximal and distal radial-scaffold junction and the new bone formation was not completed left the radial bone nonunion (Figure 9B). Gross examination of group C rabbits (implanted with 5211$_{GTA+Alginate}$), revealed that the clinical union was noticed in all the rabbits without pain in mobility over the distal and proximal radial-scaffold junction. The complete new bone formation was observed filling the defect area and the new bone tissue

bridging the defect of the radial bone was hard and the margin was distinguishable at 8 weeks post-implantation (Figure 9C,10 (A-D)). Gross examination of group D rabbits (implanted with scaffold 5211$_{PLA}$), showed similar observation as in group B but the clinical union was observed that the rabbits exhibit painless mobility over the distal radial-scaffold junction and the new bone formation was not completed left the radial bone nonunion (Figure 9D). Comparatively majority of the empty defects that were not implanted with scaffolds (control group (A)), the nonunion was observed in all the rabbits with pain mobility over the junction of radial-scaffold implant (Figure 9A). Some degree of closure of the defect site though this sites felt soft when palpated and only partial repair was observed in the radial bone defect with a thin bone formation. The empty defect sites without an implant however showed the presence of a shiny white semi-transparent tissues filling up the defect site that looked radiolucent when held up against a light source that clearly defined the defect margins upon decalcification process.

4. Discussion

Due to clinical needs and the significant of large allografts in large segmental and weight-bearing bone deformity,
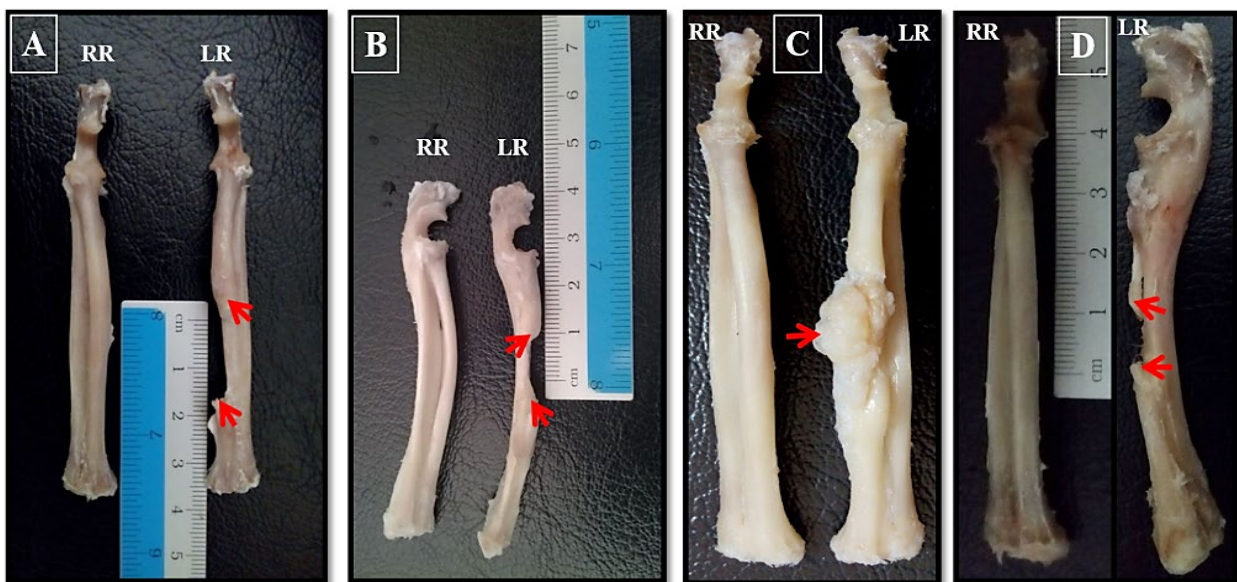

Figure 9 (A-D). Gross photographs of the radial bone of group A (control group) (A), group B (B) implanted with scaffold 5211, group C (C) implanted with scaffold 5211$_{GTA+Alginate}$ and group D (D) implanted with scaffold 5211$_{PLA}$ after 8weeks post-implantation show the new bone formation.
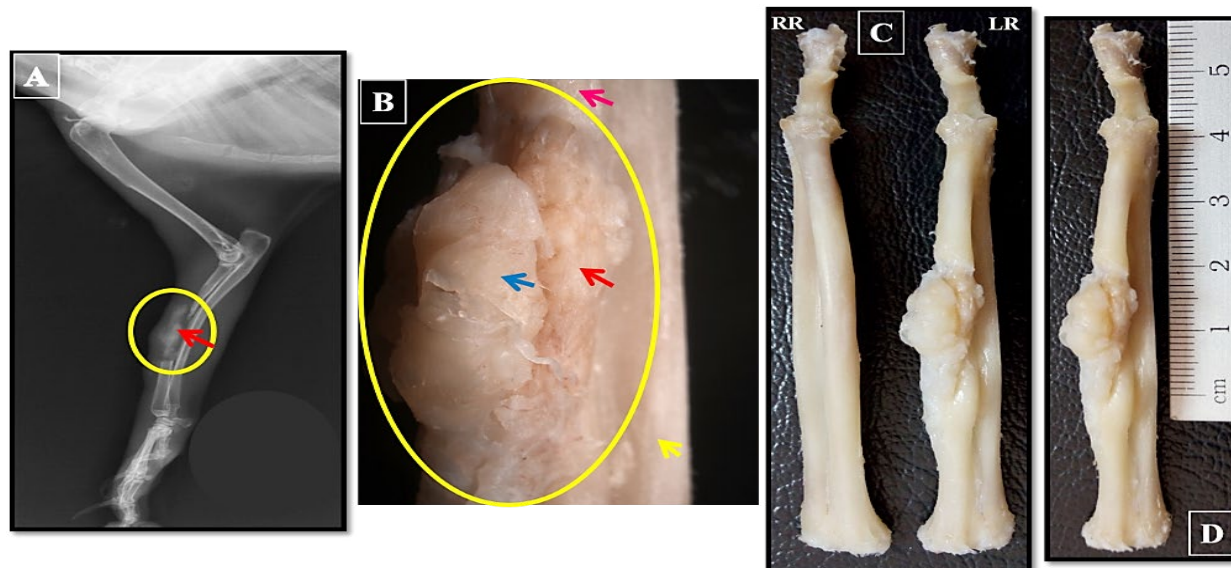
Figure 10 (A-D). Gross photographs of the radial bone of group C implanted with scaffold $5211_{GTA+Alginate}$ after 8weeks post-implantation show the new bone formation filled the part of the defect area of the radial bone (A) (yellow circle and red arrow) lateral view, stereomicroscope photograph of the radial bone (B) (lateral view) shows the new bone formation filled the part of the defect area of the radial bone (pink arrow) but without remodeling (blue and red arrows), ulna bone (yellow arrow).

this study was initiated. The challenges with the usage of large allografts are well recognized, as are the long-term problems of metal prostheses used in salvaging limb surgery[23].

In this study, novel nanocomposite scaffolds were produce for the purpose of bone replacement. Pores were produced into and onto the scaffolds surface using freeze drying technique and controlled using copolymer coating; this was done in effort to increase incorporation of bone and mechanical interconnection. The properties of the scaffolds were tailored though considering the weakening consequence of the perviousness to the scaffolds structure and biomechanically verified to meet up with the properties of the bone. This study examined the biological reactions to new nanocomposite scaffolds *in vitro* (unpublished data) and *in vivo* settings. The current study gives an insight on the actual tissue response towards the developed nanocomposite scaffolds when used as a bone implant material. The primary aim of the *in vivo* study was to evaluate tissue biocompatibility as an extended observation in order to support excellent cell biocompatibility as proven through *in vitro* evaluation conducted earlier (unpublished data). Alternatively, the ability of the developed nanocomposite scaffolds to promote the healing of the bone defect and the quality of its healing is a crucial

factor taken into consideration in this part of the study. This is mainly due to the fact that the scaffolds developed and used in the current study are neither incorporated with any form of growth promoting factor nor seeded with stem cells or bone marrow aspirates as traditionally done with the newer generation of bone scaffolds.

Experiments using animal model is very vital to develop new medical device or scaffold that can be used in human. Animal model that is excellent could exhibit the disadvantages of a procedure or scaffolds and reduce the dangers before proceeding to testing in human, nonetheless animal test outcome (durability, biocompatibility, or biomechanical strength) cannot be straight applied to human being. Selecting an appropriate animal model for a bone segment defect is difficult[11]. Rabbits possess greater speed/acceleration when moving (running or jumping), which lead to greater biomechanical pressure (bending/shearing) on their limbs, providing information about the exhaustion resistance/robustness of the material[24]. Within six months, rabbit matures and their maintenance is easy, and they can be accommodated very well in a single house. These realities made rabbits an excellent model for a segment defect model. Other studies have shown that animal model recommends the use of adult rabbits; this is to avoid epiphyseal slipping[25]. This study

choose only male rabbits to avoid hormonal fluctuation that can result to effect on bone healing and also for sex standardization. As a result of these 8-11 months old rabbits were used in this work.

This study used the radius because is easily reachable; no fixation is required due to support from the ulna, and also short period of fracture restoration in rabbit model. Cross-sectional structure of the radial bone in a rabbit's body is rounded trigonal. The cortexes are somewhat thin nonetheless strong, not easily breakable and have a large medullary cavity[24]. Critical size bone deformity (CSD) usually doesn't heal when abandon unattended to, therefore we utilize this size of defect to show that new developed scaffolds could be utilize in treating large bone defect. It is well established that the dimension of the CSD in long bone is double the bone width, and bone defects of 20 millimeters were used in this study.

Newly developed bone scaffolds such as the one in the current study and those reported by[26-28] and others are often tested for their initial biological performance without a comparative scaffold. This is likely due to the high cost of an autologous graft as well as the lack of an established commercial bone grafting material that could be used as a standard or as a positive control for the research design.

During the experimental period, all animals remained in good health and showed no signs of wound or surgical complications. The redial bone defects were periodically evaluated through radiographic imaging in which a satisfactory healing were noted by week 8 post-implantation that was eventually determined as the end point of the experimental duration. The consequent radiographs taken at day 1 and week 4 and 8 after implantation revealed the smooth unambiguous unification signal. Hence we conclude that the 8th week group would be appropriate and suitable in giving better outcome of this new scaffold which is produced for bone repairing process substitute. Complete radial bone union and healing duration in large defect of 20 millimeters was apparent at 8th week after implantation.

Outcomes of the new bone formation of the radial bone implant using radiograph presented at the center and margin of the defect implanted with non-seeded 5211, $5211_{GTA+Alginate}$ and 5211_{PLA} scaffolds was diffuse at the center and margin region of the implanted scaffold demonstrating the osteogenesis. The freshly fashioned bone image in the defect implanted with non-seeded $5211_{GTA+Alginate}$ scaffold was detectable entirely linking the

radial bone defect, and the bone formation was quicker than the preceding studies for the tissue engineering of bone repair[29]. These observations were also noted in animals in the control scaffold group with varying degree of healing. A majority of the radiographic images of the empty defect in the left limb of the animals showed complete closure of the defect site of those of the animals that implanted with $5211_{GTA+Alginate}$. The outcomes of this research revealed that the stability, bioactivity and osteoconductivity of the scaffolds are present in radial bone defect in repairs.

As noted in the radiographic images, the gross specimens obtained post euthanasia also showed complete closure of the defect in the empty defect site. The nanocomposite $5211_{GTA+Alginate}$ scaffold implanted defect however, showed good correlation to the radiographic images in terms of new bone tissue formation which were found to be healing from the defect center as a clear sign of remodeling at the interface of the bone and scaffold towards the margins. However, The nanocomposite 5211 and 5211_{PLA} scaffolds implanted defect showed good correlation to the radiographic images in terms of new bone tissue formation which were found to be healing from the defect margins as a clear sign of remodeling at the interface of the bone and scaffold towards the center cavity and was not found to have completely closed at the center cavity in animals implanted by 5211 scaffold and at the center cavity toward the distal part in animals implanted by 5211_{PLA} scaffold.

Evaluation of ALP and Ca^{+2} were carried out from sample of blood taken during the experiment in this study. It appears that the concentration of ALP in entire scaffolds of group B, C and D revealed that the secretion of ALP arises from osteoblast cells that are active. ALP is an enzyme membrane of osteoblasts and its action rises gradually as the osteoblast differentiation and maturation advance[30]. Studies have revealed that when osteoblast cells were implanted, the appearance of ALP activity was seen after 2 weeks and Ca^{+2} was noticed after 3 weeks[15,16]. Elevation of serum ALP could be as a result of speedy growth of bones, as it is produced from bone forming cells known as osteoblasts. The ALP level of groups B, C and D throughout 4-8 weeks after implantation was sustained low in comparison ALP level in group A (control group). High concentration of Ca^{+2} elicits osteoblasts to secrete ALP, which rises PO^{-4} ions concentration the locally. High PO^{-4} concentration excites additional rise in Ca^{+2} concentration where mineralization started.

Osteoblasts discharge small matrix vesicles contain ALP and pyrophosphatase that cleave PO^{-4} ions from other molecules of the matrix at the period of high extracellular Ca^{+2} and PO^{-4} concentration[31]. Assessment of ALP also revealed a high osteogenic capacity from a week after implantation. At weeks 4 and 8 after implantation the results showed that freeze dryer non-coated, coated and non-seeded scaffolds were capable of promoting osteoblastic actions, therefore the success of early formation of bone should assist the speedy bone deformity repair, thus permitting fast healing which allows daily activities[32]. This experiment revealed that there was significant difference ($P<0.05$) between treated groups and group A (control group). This revealed that the scaffold of group C and D is better than those in group B, since ALP concentration was typically higher in group A.

The concentration of Ca^{+2} could be mobilized to enter an adjacent capillary or it can be taken from the blood to deposit in the new bone matrix as required. Accumulation of Ca^{+2} by matrix vesicles (MV) was formed through osteoblasts that rise in connection with regeneration level of bone. Local isoelectric point to increase is due to matrix vesicles that accumulate Ca^{+2} and cleave PO^{-4} ions which lead to crystallization of $CaPO_4$ in the adjoining matrix vesicles. Hence, the CaPO4 crystals start matrix mineralization through development and deposition of [Ca10(PO4)6(OH)2] (hydroxyapatite) crystals in the matrix surrounding the osteoblasts that was displaying during bone formation period at the level of Ca^{+2} elevation[15,16].

Gross examinations conducted visually as well as through the stereomicroscope however showed a healthy appearance of the redial bone as well as a properly healing wound without signs of degeneration, osteolysis or inflammation. The absence of inflammation or signs of unwanted tissue reactions allows the classification of a developed scaffolds nanocomposite material as an appropriate bone substitution material that facilitates cell attachment and growth[30].

From the *in vivo* evaluation it was observed that the use of the developed nanocomposite scaffold proved to provide a better guided growth for the cells in reconstructing a proper functional tissue in a three dimensional pattern. Comparing the developed nanocomposite scaffold to some literature findings, a positive outcome could be deduced. A study by[34] on comparative performance of three ceramic bone graft substitutes that are commer-

cially available on similar kind of osseous injury defect showed neither of the bone graft substitutes performed well although claimed to be osteoconductive in nature between the study duration of 6 to 12 weeks. The author attributed the poor performance of the grafts to various possible factors including lack of persistent osteoconductiveness, destabilization of bone tissues due to early stage scaffold disintegration as well as elevated levels of inflammatory reaction towards the degrading grafting materials. Findings from this literature showed that the importance of the degrading behavior of a material in determining the ultimate healing outcome and inflammatory response in which a controlled rate of degradation positively impacts the advancement of repair.

Issues of safety are very vital with biomaterials and medical devices. The entire new materials and material combinations is very essential to be cautiously certified as regard biocompatibility and risk analysis associated to the materials has done before continuing with the clinical investigation of the materials.

Similarly, a sufficient structural property and stability as well as material composition are another crucial factor that determines the osteoconductive behavior of the grafting materials. The developed nanocomposite scaffold was found to display these favorable characteristics with a degrading behavior that was found to be in parallel to tissue formation as well as lack of any form of adverse inflammatory reaction by the host tissues towards the degrading materials. The excellent osteoconductive nature of the nanocomposite scaffolds discussed earlier in regards to recruitment of osteoblast cells and vascularization further proves that a stable osteoconductive material has potentials in supporting faster rate of new blood vessel formation and a more rapid rate of bone maturation as suggested and discussed by the author earlier as well (accepted data for publication).

The cockle shell-derived $CaCO_3$ aragonite nanocomposite porous 3D scaffolds proved to be versatile and effortlessly adjusted to meet the diverse biomechanical necessities of medical implants. Scaffolds as an implant are sufficient to withstanding the cycling loading by the patient or host animal. Also the present outcomes revealed that at 8 weeks after implantation, the deformed site was entirely joined through the new bone. Therefore, the novel cockle shell-derived $CaCO_3$ aragonite nanocomposite non seeded $5211_{GTA+Alginate}$ scaffold developed in this study are better for bone repair.

5. Conclusion

The excellent biocompatibility and osteoconductive potentials exhibited by the developed nanocomposite scaffold is an important factor that facilitates the higher degree of bone formation and remodeling giving rise to a better quality of bone formation. The *in vivo* response observed through this study possibly points to the importance of the chemical composition, structural design and coated framework of the developed scaffold in promoting good osteointegration of the scaffold material with the host tissues giving rise to a potentially workable bone scaffold material. The study also further emphasizes the potential use of natural biomaterials that are abundantly available in a relatively cost effective way that could be utilized for the possible development of excellent tissue engineered materials. Though it is impossible to mimic nature's creation, the abundance of these biomaterials available together with the ever advancing field of scientific research opens up wider avenues for the creation of materials that could closely resemble the actual biological system. The currently developed nanocomposite scaffold is one such construct with promising potentials of the third generation based grafting material in the field of bone tissue engineering.

Authors' Contributions

All authors read and approved the final manuscript.

6. Acknowledgements

Conflict of Interests

The authors state that there is no conflict of interests about the publication of this paper.

7. References

1. Yannas IV. Tissue and organ regeneration in adults. New York: Springer. 2001.
2. Janicki P, Schmidmaier G. What should be the characteristics of the ideal bone graft substitute? Combining scaffolds with growth factors and/or stem cells. Injury. 2011; 42:S77-81. crossref PMid:21724186.
3. Mistry AS, Mikos AG. Tissue Engineering Strategies for Bone Regeneration. Advances in Biochemical Engineering/Biotechnology. 2005; 94:1-22. crossref PMid:15915866.
4. Reichert JC, Saifzadeh S, Wullschleger ME, Epari DR, Schutz MA, Duda GN, Schell H. The challenge of establishing preclinical models for segmental bone defect research. Biomaterials. 2009; 30(12):2149-63. crossref. PMid:19211141.
5. Haugh MG. The development of novel scaffolds for tissue engineering with a range of structural and mechanical properties. PhD. University of Dublin. Trinity College Dublin. 2009.
6. Langer R, Vacanti JP. Tissue Engineering. Science. 1993; 260:920-6.
7. Rose FR, Oreffo RO. Bone tissue engineering: Hope vs. hype. Biochemical and Biophysical Research Communications. 2002; 292:1-7. crossref.PMid:11890663.
8. Atala A. Engineering organs. Biotechnology. 2009; 20:575-92. crossref.
9. Lind M, Bunger C. Factors stimulating bone formation. European Spine Journal. 2001; 10:S102-9. crossref. PMid:11716006 PMCid:PMC3611553.
10. Bragdon CR, Doherty AM, Rubash HE, Jasty M, Li XJ, Seeherman H, Harris WH. The efficacy of BMP-2 to induce bone in growth in a total hip replacement model. Clinical Orthopaedic. 2003; 417:50-61.
11. ISO. International Organization for Standardization. Nanotechnologies Vocabulary Part 1: Core Terms TS. 2010; 8000:4-1.
12. Vitte J, Benoliel AM, Pierres A, Bongrand P. Is there a predictable relationship between surface physical-chemical properties and cell behaviour at the interface? European Cells and Materials. 2004; 7:52-63. crossref. PMid:15389394.
13. Young S, Wong M, Tabata Y, Mikos AG. Gelatin as a delivery vehicle for the controlled release of bioactive molecules. Journal of the Controlled Release. 2005; 109:256-74. crossref. PMid:16266768.
14. Azami M, Mohammad R, Fathollah M. Gelatin/hydroxyapatite nanocomposite scaffolds for bone repair. Society of Plastic Engineers (SPE). 2010; p.1-3.
15. Zuki AB, Bahaa FH, Noordin MM. Cockle shell-based biocomposite scaffold for bone tissue engineering. Regenerative Medicine and Tissue Engineering: Cells and Biomaterials. 2011; p. 365-90.
16. Bharatham H, Zuki ABZ, Perimal EK, Loqman MY, Hamid M. Development and Characterization of Novel Porous 3D Alginate-Cockle Shell Powder Nanobiocomposite Bone Scaffold. BioMed Research International. 2014; p.1-12. crossref. PMid:25110655 PMCid:PMC4109673.

17. Kikuchi M, Matsumoto HN, Yamada T, Koyama Y, Takakuda K, Tanaka J. Glutaraldehyde cross-linked hydroxyapatite/collagen self-organized nanocomposites. Biomaterials. 2004; 25:63-9. crossref.

18. Zeltinger J, Sherwood JK, Graham DA, Mueller R, Griffith LG. Effect of pore size and void fraction on cellular adhesion, proliferation and matrix deposition. Tissue Engineering. 2001; 7:557-72. crossref. PMid:11694190.

19. Hum J, Luczynski KW, Nooeaid P, Newby P, Lahayne O, Hellmich C, Boccaccini AR. Stiffness improvement of 45S5 bioglass ® - based scaffolds through natural and synthetic biopolymer coating: An Ultrasonic study. Strain. 2013; 49:431-9. crossref.

20. Govindan R, Kumar GS, Girija EK. Polymer coated phosphate glass/hydroxyapatite composite scaffolds for bone tissue engineering applications. RSC Advances. 2015; 5:60188-98. crossref.

21. Pearce AI, Richards RG, Milz S, Schneider E, Pearce SG. Animal models for implant biomaterial research in bone: A review. European Cells and Materials. 2007; 13:1-10.

22. Nakagawa H, Kamimura M, Takahara K, Hashidate H, Kawaguchi A, Uchiyama S, Miyasaka T. Changes in total alkaline phosphatase level after hip fracture: Comparison between femoral neck and trochanter fractures. Journal of Orthopaedic Science. 2006; 11(2):135-9. crossref. PMid:16568384.

23. Thompson RC, Garg JA, Clohisy DR, Cheng EY. Fractures in large segment allografts. Clinical Orthopaedics and Related Research. 2000; 370:227-35. crossref. PMid:10660718.

24. Calasans-Maia MD, Monteiro ML, Ascoli FO, Granjeiro JM. The rabbit as an animal model for experimental surgery. Acta Cirurgica Brasileira. 2009; 24(4):325-8. crossref. PMid:19705034.

25. Herold GH, Hurvitz A, Tadmor A. The effect of growth hormone on the healing of experimental bone defects. Acta Orthopaedica Scandinavica Journal. 1971; 42(5):377-84. crossref.

26. Gonzalez-Toro DC, Thayumanavan S. Advances in polymer and polymeric nanostructures for protein 17 conjugation. European Polymer Journal. 2013; 49:2906-18. crossref. PMid:24058205 PMCid:PMC3775383.

27. Diaz-Rodriguez P, Gonzalez P, Serra J, Landin M. Key parameters in blood-surface interactions of 3D 19 bioin-spired ceramic materials. Materials Science and Engineering C. 2014; 41:232-9. crossref. PMid:24907756

28. Vasconcellos LMR, Leite DO, Oliveira FN, Carvalho YR, Cairo CAA. Evaluation of bone in growth into 44 porous titanium implant: Histomorphometric analysis in rabbits. Brazilain Oral Research. 2010; 24(4):399-405. crossref. PMid:21180959.

29. Li Z, Li ZB. Repair of mandible defect with tissue engineering bone in rabbits. ANZ Journal of Surgery. 2005; 75:1017-21. crossref. PMid:16336400.

30. Jin HH, Kim DH, Kim TW, Shin KK, Jung JS, Park HC, Yoon SY. In-vivo evaluation of porous hydroxyapatite/chitosan-alginate composite scaffolds for bone tissue engineering. International Journal of Biological Macromolecules. 2012; 51(5):1079-85.

31. Whited BM, Whitney JR, Hofmann MC, Xu Y, Rylander MN. Pre-osteoblast infiltration and differentiation in highly porous apatite-coated PLLA electrospun scaffolds. Biomaterials. 2011; 32(9):2294-304. crossref. PMid:21195474.

32. Sikavitasa VI, Bancroft GN, Lemoine JJ, Liebschner MAK, Dauner M, Mikos AG. Flow perfusion enhances the calcified matrix deposition of marrow stromal cells in biodegradable nonwoven fiber mesh scaffolds. Annals of Biomedical Engineering. 2005:33(1):63-70. crossref.

33. Ross MH, Pawlina W. A text and atlas with correlated cell and molecular biology. 5th edition. 2006; p. 224-5. PMCid:PMC1978070.

34. Hing KA, Wilson LF, Buckland T. Comparative performance of three ceramic bone graft substitutes. The Spine Journal. 2007; 7(4):475-90. crossref. PMid:17630146.